

Channeling contrast microscopy of epitaxial lateral overgrowth of ZnO/GaN films

Hailong Zhou^a, Hui Pan^a, Taw Kuei Chan^a, Chee Sheng Ho^a, Yanping Feng^a,
Soo-Jin Chua^b, Thomas Osipowicz^{a,*}

^a Department of Physics, National University of Singapore, 2 Science Drive 3, 117542 Singapore, Singapore

^b Institute of Materials Research and Engineering, 3 Research Link, 117602 Singapore, Singapore

Available online 14 February 2007

Abstract

As a wide band gap (3.37 eV) semiconductor, ZnO is of great interest for applications in opto- and nano-electronics, as technologies of synthesis for ZnO layers are developed. It has been reported that the blue-UV generation can be realized in ZnO thin-films, ZnO whiskers, p-type ZnO films and thin-film diode structures at room temperature. Zinc oxide crystal of high quality with a reduced number of crystal defects can be grown on a sapphire substrate. The density of dislocations can be decreased by orders of magnitude using epitaxial lateral overgrowth (ELO), which employs a SiO₂ mask layer to act as a stop layer for dislocations in so called wing areas.

Rutherford Backscattering Spectrometry (RBS) is a powerful tool for the quantitative characterization of the depth profile and the crystallinity of such structures, and channeling contrast microscopy (CCM), which employs a focused ion beam in order to obtain laterally resolved channeling yield data, is ideally suited to determine micro structural characteristics, (e.g. defect densities, tilts in lattice planes, strain) of such samples. Here we report results from proton channeling contrast measurements of laterally overgrown ZnO thin films. The results show that high crystal quality ZnO films can be grown using the ELO method. Cross-sectional scanning electron microscopy (SEM), high resolution transmission electron microscopy (HRTEM) and CCM are used to study the morphology and micro-structure of the ELO ZnO films.

© 2007 Elsevier B.V. All rights reserved.

PACS: 74.78.Fk; 61.85.+p; 82.80.Yc

Keywords: ZnO; Epitaxial lateral overgrowth; Ion channeling analysis; Channeling contrast microscopy

1. Introduction

Zinc oxide (ZnO), a representative group II–VI compound semiconductor with a direct wide bandgap of 3.37 eV and large exciton binding energy of 60 meV at room temperature, has attracted considerable attention over the past years owing to its attractive properties, such as good piezoelectric characteristics, chemical stability, and biocompatibility, etc., and its potential applications in optoelectronic switches, high-efficiency photonic devices,

and near-UV lasers, and for assembling complex three dimensional nanoscale systems [1–4].

In most reported work, sapphire has been used as the substrate to produce epitaxial ZnO films [5–7]. The quality of such films is difficult to optimize due to the high lattice mismatch between sapphire and ZnO (about 14%). Recently, Vispute et al. have reported the epitaxial growth of ZnO on GaN/sapphire substrates [8]. Such a method can significantly improve the quality of ZnO films because the lattice mismatch is within 1.9%. However, because of the high dislocation density (around 10⁹–10¹⁰ cm⁻²) in the GaN grown on c-sapphire, the as-grown ZnO films on c-GaN are known to contain higher defect densities, which are mainly threading dislocations. Epitaxial lateral

* Corresponding author.

E-mail address: phyto@nus.edu.sg (T. Osipowicz).

overgrowth (ELO) was designed in order to reduce the density of threading dislocations in GaN thin films [9–11]. GaN films with high crystalline quality and low dislocation density can be obtained based on this technique, leading to the improvement of the performance of GaN-based devices. An ELO-GaN-based blue laser diode with a lifetime longer than 10,000 h has been realized [12]. Furthermore, despite significant progress on ZnO films and nanostructures, the difficulty of p-type doping in ZnO has impeded the fabrication of ZnO p–n homojunction devices. As an alternative approach to homojunction, an n-ZnO/p-GaN heterojunction has been suggested as a strong candidate for device applications [13].

X-Ray diffraction studies are used to measure wing tilt with the scattering plane perpendicular to the stripe direction [14–16]. However, this technique is unable to provide laterally resolved information of the crystallographic tilts across the GaN stripes. Recently, we reported the use of channeling contrast microscopy (CCM) to image crystallographic tilts in micron sized overgrown regions of LEO GaN, using a 2-MeV alpha particle beam with a sub-micron spot-size [17]. Rocking curves measured perpendicular to the GaN stripes reveal the wing tilt relative to the window region. Here we report results from the 2-MeV proton beam CCM measurements of laterally overgrown ZnO thin films. A proton beam is, in certain cases, the preferable probe, because of its larger range and its smaller critical angle, e.g. for thicker samples with regions inaccessible with alpha beams.

2. Experimental details

In the preparation for ELO GaN, a 2 μm GaN film was first deposited by metal organic chemical vapor deposition (MOCVD) system on a c-plane sapphire substrate with low temperature GaN as buffer layer. Trimethyl-metals and ammonia (NH_3) were used as sources of Ga and N with H_2 as carrier gas. A 100 nm SiO_2 mask was patterned into stripes oriented in the GaN $[1\bar{1}00]$ direction, defining a 5 μm wide opening with a period of 13 μm . ELO GaN layers were grown by controlling the facet planes via choosing the growth temperature and the reactor pressure by facet control epitaxial lateral growth (FACELO) [18,19]. The growth temperature and reactor pressure were 1000 $^\circ\text{C}$ and 200 Torr, respectively. After that, the ELO GaN/sapphire substrates were put into a tube furnace to grow the ZnO films by thermal vaporization and condensation of Zn (99.99% purity) in the presence of oxygen. The alumina boat with Zn powder was placed at the center of a quartz tube and purged with a Helium (99.999% purity) flow with 100 standard cubic centimeters per minute (sccm). The furnace temperature was increased to growth temperature, and an oxygen (99.99% purity) flow was introduced into the tube reactor. The mixed O_2 and He gas was maintained throughout the whole reaction process, which normally takes 30 min.

The ZnO/GaN/sapphire layers were studied with Scanning Electron Microscopy (JEOL JSM-6700F, 5 kV),

transmission electron microscopy (Philips CM300, 300 kV) and Channeling contrast microscopy (Set up by Center for Ion Beam Application at the National University of Singapore with a 3.5 MeV singletron accelerator). CCM was used to image the micron sized overgrown regions of ELO ZnO, using a 2-MeV proton particle beam with a sub-micron spot-size. Channeling RBS spectra were recorded with 300 mm^2 PIPS detector with 19KeV energy resolution at a scattering angle of 145° , and micro PL system (Renishaw, the PL spectra were recorded using a 325 nm excitation line with a lateral resolution of 2.0 μm).

3. Results and discussion

Fig. 1(a) shows the cross-sectional SEM image of ZnO film grown on ELO GaN template. The ELO GaN grown along the $[1\bar{1}00]$ direction, and $\{11\bar{2}2\}$ sidewall facets is clearly displayed. It is known that the morphology of ELO GaN varies with the different growth condition. Two-layer ZnO/GaN structure is found on the sapphire

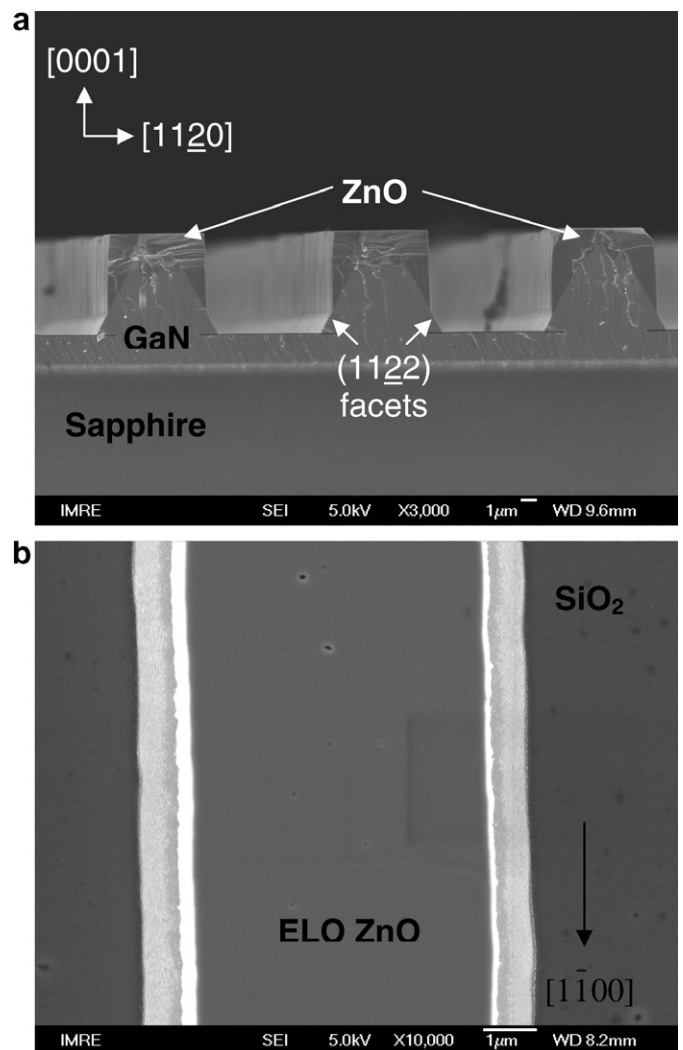


Fig. 1. (a) Cross-sectional SEM of the ZnO/ELO GaN on the sapphire substrate; (b) Top view SEM image of the ZnO/ELO GaN, the circles show the pit defects found in the ELO ZnO surface.

substrate. Besides the original GaN stripes, an extra layer is found grown on the top with uniform thickness on a large scale. It can be seen that the original serrated ELO GaN stripe has a height of $5\ \mu\text{m}$ and a width of $7\ \mu\text{m}$. After ZnO growth, the near rectangle shape is observed with a width of about $6.2\ \mu\text{m}$, indicating that the significant lateral growth of ZnO occurred on the ELO GaN and the faster growth facet is $(1\ 1\ \bar{2}0)$. No extra layers were found on the SiO_2 mask layer, which indicated that the ZnO top layer was selectively grown on the ELO GaN template. Such morphology originates from the different growth mode between the ELO GaN and the c-GaN surface. Fig. 1(b) shows the top view of the sample after ZnO grown on the GaN template, pit defects can be found on the surface of the top layer, which may come from threading dislocation propagating from the ELO GaN into the ZnO films.

The microstructure of the top layer and the nature of epitaxial growth of the ZnO films on ELO GaN were investigated by high resolution TEM (HRTEM). Fig. 2 shows the typical HRTEM image of the ZnO/ELO GaN interface, from which it can be seen the lattice fringes of ZnO are perfectly aligned with those of ELO GaN and the interface is sharp on the atom level. The corresponding selective area electron diffraction (SAED) pattern is shown in the inset. Only one set of SAED pattern is observed, resulting from the very close lattice parameters between ZnO and GaN hexagonal structures. The pattern also verifies the perfect epitaxial growth of ZnO on GaN and their high crystal quality.

A cross-sectional TEM image with lower magnification of the ZnO/ELO GaN interface is presented in Fig. 2(b). The ELO GaN dislocations have been studied by several groups [20,21] and the formation of the horizontal dislocations (HDs) is very important due to the fact that HDs can dramatically decrease the thread dislocations (TDs) density in the regrown GaN regions. From the point of view of the dislocation line tension, any dislocation would tend to become perpendicular to a free surface to diminish its energy. As a result, dislocations would gradually change their line directions towards the normal direction of the current facet plane, as can be seen in Fig. 2(b). High quality wing regions have been realized by the growth of ZnO $(1\ 1\ \bar{2}0)$ vertical sidewalls.

As shown in Fig. 3(a), bands of high and low scattering intensity with a periodicity of $13\ \mu\text{m}$ are found in the RBS channeling contrast microscopy (CCM) maps. In this technique a focused $2\ \text{MeV}\ \text{H}^+$ beam is used to obtain laterally resolved channeling yield data. The bands correspond to different regions of the ELO ZnO, and they are designated as band 1 (ELO ZnO region) and band 2 (voids between the ELO ZnO region) as shown in Fig. 3(a). All data were collected in list-mode, therefore, it is possible to extract separate spectra from band 1 and band 2 (as defined in Fig. 3(a)). Laterally resolved channeling data have been extracted from the RBS spectra in near-surface regions. Fig. 3(b)–(d) shows random and channeled spectra of the

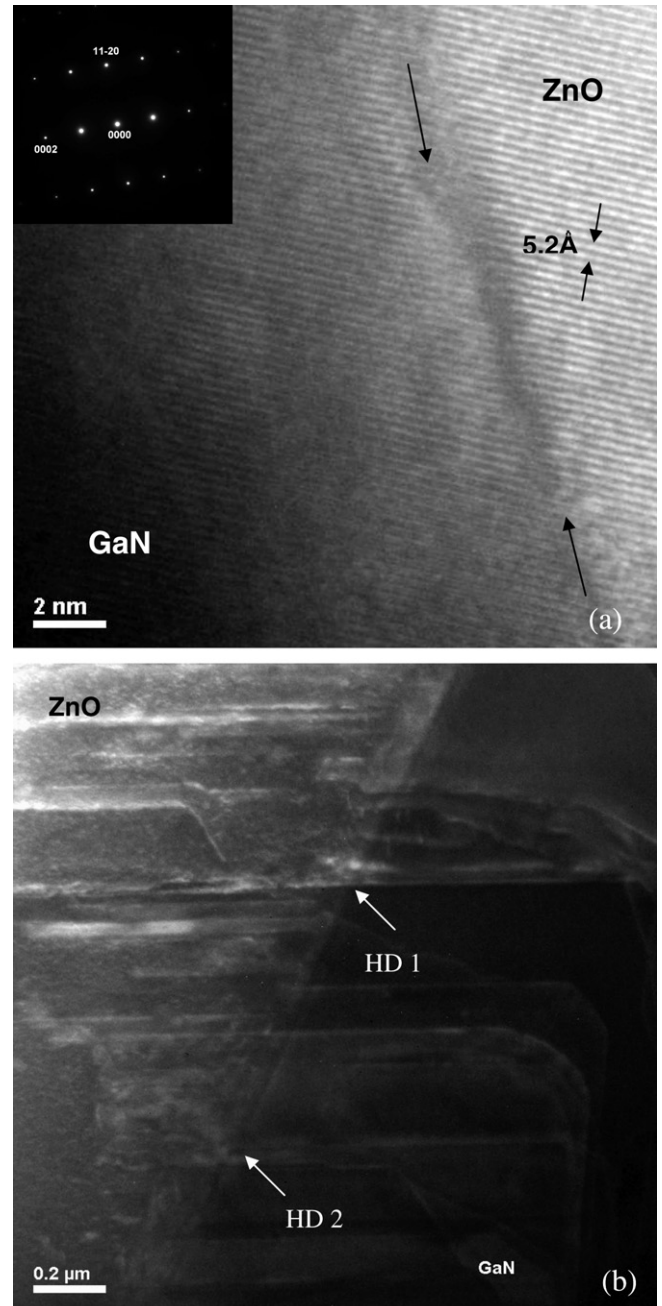


Fig. 2. (a) HRTEM image and the corresponding SAED pattern of ZnO/ELO GaN interface grown at $800\ ^\circ\text{C}$ with the oxygen flow rate $10\ \text{sccm}$. (b) Cross-sectional TEM image with $g = 1\ \bar{1}00$ near the interface of ZnO/ELO GaN grown at $800\ ^\circ\text{C}$ with the oxygen flow rate $10\ \text{sccm}$, HDs are indicated with the arrows.

band 1 part of the ELO ZnO grown at $780\ ^\circ\text{C}$, $800\ ^\circ\text{C}$ and $820\ ^\circ\text{C}$, respectively, with the oxygen flow rate of $10\ \text{sccm}$, for channeling and random alignment of the beam. $A\chi_{\text{min}}$ (the minimum ratio of the intensity of channeling spectra to random) of 5% is obtained for axial $[0001]$ channeling of the ELO ZnO grown at $800\ ^\circ\text{C}$. The full lines represent XRUMP [22] fits of the random spectra, they were generated by averaging the simulated RBS spectra of the structures, as deduced from the SEM data. Clearly, the lowest χ_{min} is obtained from the $800\ ^\circ\text{C}$

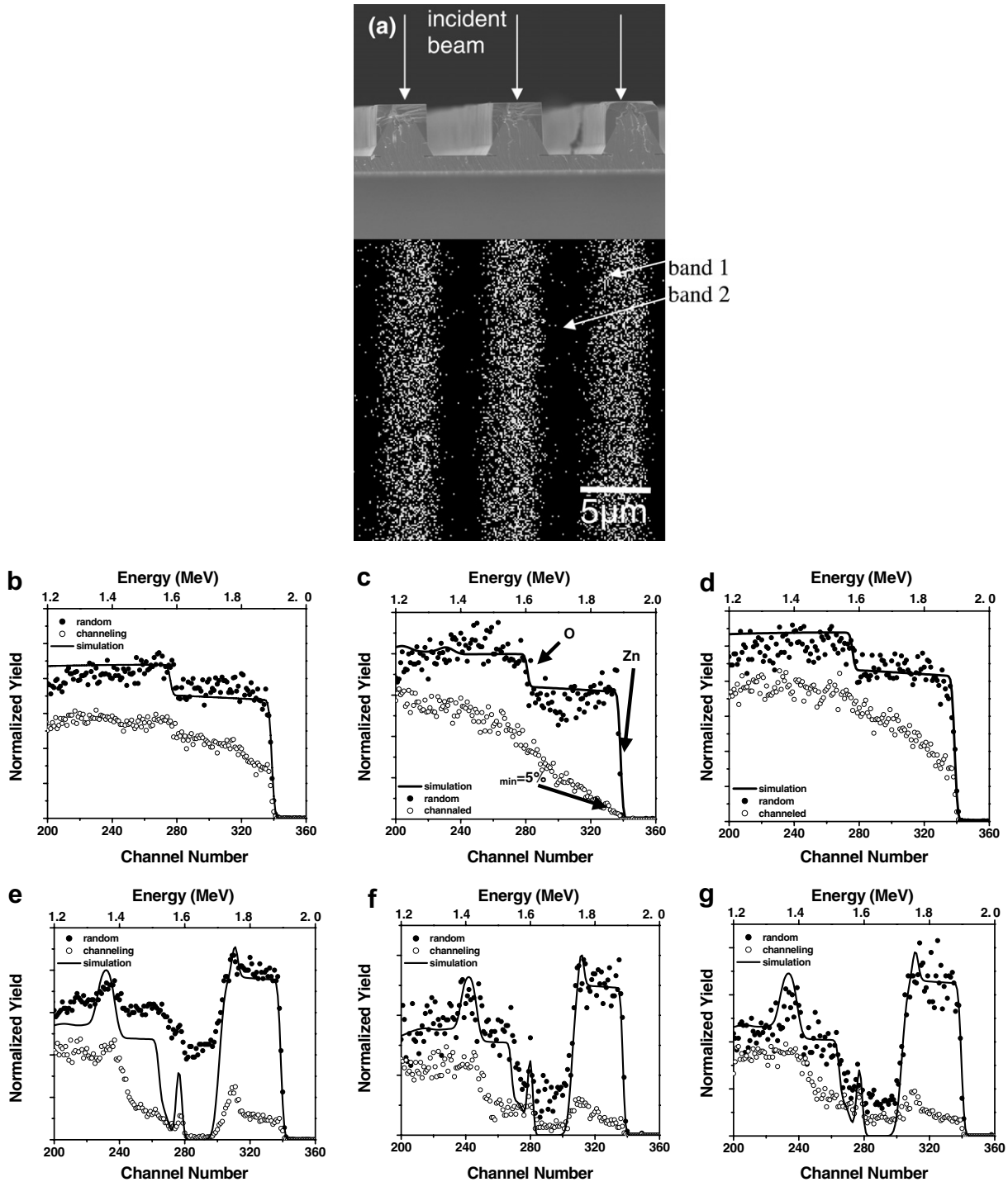


Fig. 3. (a) Origin of the contrast pattern observed in the CCM maps; (b), (c) and (d) are RBS spectra of band 1 region random and [0001] channelled ZnO/ELO GaN grown at 780 °C, 800 °C and 820 °C, respectively, with the oxygen flow rate 10 sccm; (e), (f) and (g) are RBS spectra of band 2 area random and [0001] channelled ZnO/ELO GaN grown at 780 °C, 800 °C and 820 °C, respectively, with the oxygen flow rate 10 sccm.

growth samples. This indicates that the ELO ZnO grown at 800 °C with an oxygen flow rate of 10 sccm has excellent crystal quality, much better than the sample grown at 820 °C. Fig. 3(e)–(g) show random and channelled spectra of the band 2 part of the 780 °C, 800 °C and 820 °C ELO ZnO, the 2 μm GaN buffer layer is clearly seen with the random spectra.

The optical properties of the ZnO layers on ELO GaN were investigated by room temperature micro-PL spectroscopy. Fig. 4, the ratio of GaN peak intensity to that of ZnO is seen to vary with the temperature, indicating different thickness or/and crystal properties of ELO ZnO layers. In the PL spectra (Fig. 4), the peaks from GaN and ZnO can be seen around 363 and 380 nm, respectively. From

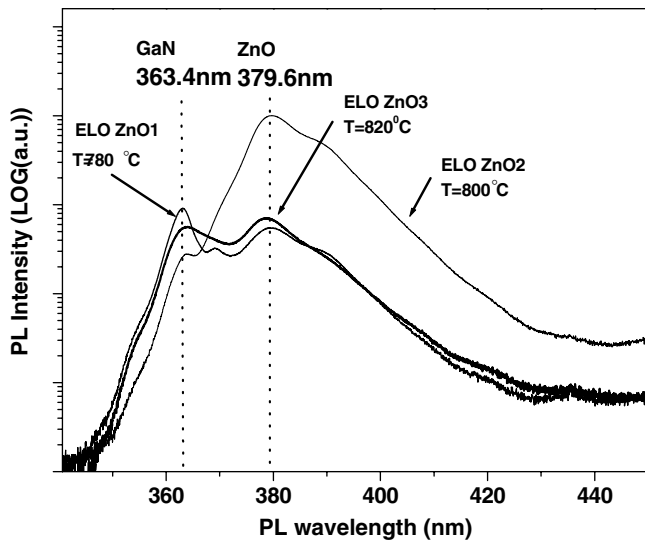


Fig. 4. (a) The micro-PL spectra were taken from three different ZnO/ELO GaN samples grown at different temperature with the same oxygen flow rate of 10 sccm, excitation by 325 nm laser with a power of 1 mW.

the spectra of 780 °C ELO ZnO/GaN sample, the GaN/ZnO intensity ratio of larger than one may suggest that the thickness of the ELO ZnO layer is no larger than 300 nm or the as grown ZnO is the nano rods, as observed from the SEM images. The strongest PL intensity of the ELO ZnO is observed from the 800 °C grown ELO ZnO/GaN with the full width at half maximum (FWHM) of the ZnO peak of about 5.5 nm, which is the narrowest of three ELO ZnO samples from different temperatures. This implies a higher epitaxial crystalline quality of ELO ZnO films grown at 800 °C. And the spectra of 820 °C ELO ZnO/GaN shows the degraded crystalline, with the broadening of ZnO peak (around 23 nm). The PL spectra show that the best ELO ZnO quality is achieved at 800 °C, together with the oxygen flow rate of 10 sccm.

4. Conclusions

High quality epitaxial ZnO/ELO GaN heterostructures has been demonstrated on sapphire substrates. These heterostructures showed a substantial improvement in the crystalline quality with a lower defect density and excellent photoluminescence emission. In addition, the lattice matching between the ZnO and GaN, thermal and optical properties, and the perfect interfaces of these ELO ZnO/GaN heterostructures will provide new opportunities for the fabrication of hybrid ZnO/GaN optoelectronic devices on sapphire.

Acknowledgements

The authors acknowledge support from the NUS Academic Research Fund. We would like to thank Institute Materials Research and Engineer staff Ms. Chow Shue Yin and Ms. Yong Anna Marie for their help in TEM characterization.

References

- [1] Y.N. Xia, P.D. Yang, Y. Sun, Y. Wu, B. Mayers, Y. Yin, F. Kim, H. Yan, *Adv. Mater.* 15 (2003) 353.
- [2] Z.W. Pan, Z.R. Dai, Z.L. Wang, *Science* 291 (2001) 1947.
- [3] J. Hu, T.W. Odom, C.M. Lieber, *Accounts. Chem. Res.* 32 (1999) 435.
- [4] C.S. Chen, C.T. Kuo, T.B. Wu, I.N. Lin, *Jpn. J. Appl. Phys.* 1 (36) (1997) 1169.
- [5] M. Kawasaki, A. Ohtomo, H. Koinuma, Y. Sakurai, Y. Yoshida, Z.K. Tang, P. Yu, G.K.L. Wang, Y. Segawa, *Mater. Sci. Forum* 264 (1998) 1459.
- [6] D.M. Bagnall, Y.F. Chen, Z. Zhu, T. Yao, S. Koyama, M.Y. Shen, T. Goto, *Appl. Phys. Lett.* 70 (1997) 2230.
- [7] V. Srikant, V. Sergo, D.R. Clarke, *J. Am. Ceram. Soc.* 78 (1995) 1931.
- [8] R.D. Vispute, V. Talyansky, S. Choopun, R.P. Sharma, T. Venkatesan, M. He, X. Tang, J.B. Halpern, M.G. Spencer, Y.X. Li, L.G. Salamanca-Riba, A.A. Iliadis, K.A. Jones, *Appl. Phys. Lett.* 73 (1998) 348.
- [9] B.Y. Tsaur, R.W. McClelland, J.C.C. Fan, R.P. Gale, J.P. Salerno, B.A. Vojak, C.O. Bozler, *Appl. Phys. Lett.* 41 (1982) 347.
- [10] T. Nishinaga, T. Nakano, S. Zhang, *Jpn. J. Appl. Phys.* 27 (1988) 964.
- [11] T.S. Zheleva, O.-H. Nam, M.D. Bremser, R.F. Davis, *Appl. Phys. Lett.* 71 (1997) 2472.
- [12] Gerhard Fasol, *Science* 278 (1997) 1902.
- [13] S.-K. Hong, T. Hanada, H. Makino, Y. Chen, H.-J. Ko, T. Yao, A. Tanaka, H. Sasaki, S. Sato, *Appl. Phys. Lett.* 78 (2001) 3349.
- [14] P. Fini, J.P. Ibbetson, H. Marchand, L. Zhao, S.P. DenBaars, J.S. Speck, *J. Cryst. Growth* 209 (2000) 581.
- [15] P. Fini, L. Zhao, B. Noran, M. Hansen, H. Marchand, J.P. Ibbetson, S.P. DenBaars, U.K. Mishra, J.S. Speck, *Appl. Phys. Lett.* 75 (1999) 1706.
- [16] P. Fini, A. Munkholm, C. Thompson, G.B. Stephenson, J.A. Eastman, M.V. Ramana Murty, O. Auciello, L. Zhao, S.P. DenBaars, J.S. Speck, *Appl. Phys. Lett.* 76 (26) (2000) 3893.
- [17] E.J. Teo, T. Osipowicz, A.A. Bettiol, F. Watt, M.S. Hao, S.J. Chua, *Nucl. Instr. and Meth. B* 181 (2001) 231.
- [18] H. Miyake, A. Motogaito, K. Hiramatsu, *Jpn. J. Appl. Phys.* 38 (1999) L1000.
- [19] K. Hiramatsu, K. Nishiyama, M. Onoshi, H. Mizutani, M. Narukawa, A. Motogaito, H. Miyake, Y. Iyechika, T. Maeda, *J. Crystal Growth* 221 (2000) 316.
- [20] Noriyuki Kuwano, Kayo Horibuchi, Koji Kagawa, Shigefumi Nishimoto, Manabu Sueyoshi, *J. Cryst. Growth* 237–239 (2002) 1047.
- [21] M. Ishida, M. Ogawa, K. Orita, O. Imafuji, M. Yuri, T. Sugino, K. Itoh, *J. Cryst. Growth* 221 (2000) 345.
- [22] L.R. Doolittle, Conference proceedings, Heavy Ions, MRS. 1990.